

Specific Heat Measurement of Cubic Sodium Tungsten Bronzes from 200 To 800°K

HIDEAKI INABA AND KEIJI NAITO

Department of Nuclear Engineering, Faculty of Engineering, Nagoya University

Received October 17, 1974

Specific heats of three cubic sodium tungsten bronze samples (Na_xWO_3) with x values of 0.485, 0.698, and 0.794 were measured from 200 to 800°K. Specific heats per gram-atom of three samples at the same temperature were equal within experimental error regardless of the difference of the composition and those at 700°K showed the Dulong-Petit value. λ -Type specific heat anomalies were observed around 400°K, showing the existence of a second-order phase transition. The transition temperature increases as the sodium content of the sample increases, and a linear relationship between enthalpy change of the transition and the transition temperature was observed. The entropy increments of the transition were obtained as 0.79, 0.84, and 0.90 J/mole·K for $\text{Na}_{0.485}\text{WO}_3$, $\text{Na}_{0.698}\text{WO}_3$, and $\text{Na}_{0.794}\text{WO}_3$, respectively. It is supposed that the entropy increment of the transition is caused by the increase in the number of slightly displaced atoms with respect to the ideal perovskite position.

1. Introduction

The cubic sodium tungsten bronzes have the chemical formula Na_xWO_3 , with $0.4 < x < 1.0$, and are characterized by the perovskite structure. The properties of these compounds are of interest not only because they are metallic compounds of high electric and thermal conductivity (1, 2), but also because they are nonstoichiometric compounds of metal-oxygen systems. In the nonstoichiometric compounds, the difference in stoichiometry usually has little influence on the specific heat value; however, when phase transition occurs, as in the case of Ni_{1-x}Se (3), Fe_{1-x}Se (4) and U_4O_{9-y} (5), the enthalpy and entropy changes of the phase transition depend on nonstoichiometry.

The existence of the phase transition above room temperature in the cubic sodium tungsten bronze has been suggested by the following results. Optical measurements (6) have shown the presence of a birefringent phase over a wide temperature range from

about 270 to about 420°K, depending on the sodium content of the sample. Anomalies have been observed above room temperature in the coefficient of thermal expansion (7), ^{23}Na spin-phonon relaxation rate (8), and electrical conductivity (9). DSC measurement (9) has found the change of thermal property near 420°K, and an abrupt decrease of thermal conductivity (10) has been observed between 400 and 500°K.

Gerstein et al. (11) have measured the specific heat of $\text{Na}_{0.679}\text{WO}_3$ in the range 15 to 300°K by an adiabatic calorimeter. Taylor and Weller (9) have reported the specific heat of $\text{Na}_{0.8}\text{WO}_3$ in the range 330 to 770°K by using DSC apparatus; however, their data are not precise enough because of the use of DSC apparatus.

In this paper, we have measured the specific heat of three tungsten bronzes, $\text{Na}_{0.485}\text{WO}_3$, $\text{Na}_{0.698}\text{WO}_3$, and $\text{Na}_{0.794}\text{WO}_3$, in the range 200 to 800°K, and discussed the phase transition of nonstoichiometric sodium tungsten bronzes.

TABLE I

SPECIFIC HEAT OF Na_xWO_3

2. Experimental

2.1. Sample Preparation

Na_xWO_3 samples were prepared as described by Brown and Banks (12). Na_2WO_4 , WO_3 , and W powder of chemical pure grade with no further purification were uniformly mixed in proper ratios, sealed in an evacuated quartz tube and kept at 700°C for 150 hr. Products were crushed into fine powder and annealed at 600°C for 150 hr.

Sodium concentration of the samples was determined by the measurement of the lattice parameter of X-ray diffraction using the known relation (12) between the lattice parameter and the sodium concentration. The composition of samples was determined to be $\text{Na}_{0.485}\text{WO}_3$, $\text{Na}_{0.698}\text{WO}_3$, and $\text{Na}_{0.794}\text{WO}_3$.

2.2. Specific Heat Measurement

Specific heat of Na_xWO_3 has been measured by the adiabatic scanning calorimeter (13); in this calorimeter the power supplied to the sample was measured continuously, where heating rate was controlled to be constant regardless of the kind and amount of the sample.

Heating rate was chosen as $2^\circ\text{K}/\text{min}$, and the measurement was carried out between 200 and 800°K under nitrogen gas of about 10 Torr. The heating rate control and adiabatic control were usually maintained to within $\pm 0.01^\circ\text{K}/\text{min}$ and $\pm 0.03^\circ\text{K}$, respectively. The Na_xWO_3 sample was sealed in a quartz vessel filled with helium gas at about 250 Torr. The sample amount used was 12.246 g for $\text{Na}_{0.485}\text{WO}_3$, 11.371 g for $\text{Na}_{0.698}\text{WO}_3$, and 13.185 g for $\text{Na}_{0.794}\text{WO}_3$.

3. Results and Discussion

Specific heats measured for $\text{Na}_{0.485}\text{WO}_3$, $\text{Na}_{0.698}\text{WO}_3$, and $\text{Na}_{0.794}\text{WO}_3$ are listed in Table I and are shown in Fig. 1, where the results for $\text{Na}_{0.679}\text{WO}_3$ by Gerstein et al. (11) and those for $\text{Na}_{0.8}\text{WO}_3$ by Taylor and Weller (9) are also shown for comparison. The precision of the specific heat measurement

T ($^\circ\text{K}$)	Specific heat ($\text{J}/\text{mole}\cdot\text{K}$)		
	$\text{Na}_{0.485}\text{WO}_3$ (MW; 243.01)	$\text{Na}_{0.698}\text{WO}_3$ (MW; 247.90)	$\text{Na}_{0.794}\text{WO}_3$ (MW; 250.11)
200	71.2	75.4	79.2
205	72.4	76.4	80.2
210	73.7	77.8	81.3
215	74.8	78.7	82.3
220	75.8	80.0	83.2
225	76.5	81.0	84.2
230	77.6	81.9	85.1
235	78.4	82.8	86.2
240	79.5	83.8	87.3
245	80.6	84.7	88.2
250	81.5	85.5	89.1
255	82.1	86.2	90.2
260	83.1	87.2	91.2
265	84.3	88.3	92.2
270	84.9	89.4	92.8
275	85.6	90.0	93.7
280	86.6	90.8	94.5
285	87.2	91.4	95.1
290	87.7	91.8	95.7
295	88.3	92.3	96.0
300	89.0	93.1	97.2
305	89.8	93.8	97.7
310	90.3	94.5	98.2
315	90.9	95.3	98.5
320	91.3	95.7	99.0
325	91.9	96.2	99.4
330	92.1	96.4	99.8
335	92.5	96.9	100.2
340	93.2	97.3	100.8
345	93.6	97.5	101.1
350	94.1	98.2	101.6
355	94.2	98.8	102.1
360	94.5	99.3	102.5
365	95.0	99.7	102.7
370	95.3	100.2	103.7
375	95.7	100.8	103.9
380	96.5	101.2	104.1
385	97.1	101.5	104.6
390	97.9	102.0	105.1
395	98.7	102.7	105.3
400	98.4	103.4	105.7
405	98.0	104.2	106.6
410	97.6	104.6	107.0
415	97.8	103.9	107.7
420	98.3	103.7	108.7
425	98.6	103.5	109.6
430	99.1	103.6	110.5

TABLE I—(continued)

$T^{\circ}(\text{K})$	Specific heat (J/mole·K)		
	$\text{Na}_{0.485}\text{WO}_3$ (MW; 243.01)	$\text{Na}_{0.698}\text{WO}_3$ (MW; 247.90)	$\text{Na}_{0.794}\text{WO}_3$ (MW; 250.11)
435	99.7	103.8	111.3
440	100.1	104.4	110.8
445	100.2	104.7	110.2
450	100.7	105.1	110.0
455	101.0	105.4	110.0
460	101.5	105.9	110.1
465	101.7	106.2	110.4
470	102.1	106.6	110.7
475	102.6	107.0	110.8
480	102.7	107.2	111.2
485	103.4	107.7	111.2
490	103.6	107.9	111.1
495	103.8	108.1	112.0
500	104.2	108.2	112.5
505	104.3	108.5	112.5
510	104.7	108.9	112.8
515	105.0	109.1	113.1
520	105.3	109.9	113.7
525	105.5	110.2	114.0
530	105.7	110.2	113.8
535	105.9	110.5	114.1
540	106.1	110.5	114.4
545	106.6	110.9	114.7
550	106.9	111.3	114.8
555	107.2	111.3	115.0
560	107.5	111.5	114.9
565	107.6	111.9	115.1
570	107.9	112.4	115.9
575	108.2	112.8	115.8
580	108.4	113.0	115.9
585	108.6	113.2	115.9
590	108.8	113.5	116.2
595	109.0	113.7	116.1
600	109.1	113.8	116.4
605	109.5	114.2	116.8
610	109.7	114.5	117.1
615	110.1	115.0	117.5
620	110.3	115.1	117.6
625	110.3	115.2	117.7
630	110.4	115.3	117.9
635	110.5	115.4	118.2
640	110.8	115.8	118.4
645	111.0	115.9	118.6
650	111.1	116.1	118.7
655	111.3	116.3	118.9
660	111.2	116.4	119.2
665	111.5	116.7	119.7
670	111.8	116.7	119.8
675	112.3	116.8	119.9

TABLE I—(continued)

$T^{\circ}(\text{K})$	Specific heat (J/mole·K)		
	$\text{Na}_{0.485}\text{WO}_3$ (MW; 243.01)	$\text{Na}_{0.698}\text{WO}_3$ (MW; 247.90)	$\text{Na}_{0.794}\text{WO}_3$ (MW; 250.11)
680	112.1	117.0	120.0
685	112.1	117.3	120.1
690	112.4	117.3	120.1
695	112.4	117.6	120.2
700	112.4	117.6	120.2
705	112.8	117.7	120.4
710	113.3	117.9	120.5
715	113.3	117.9	120.6
720	113.3	117.8	120.7
725	113.3	117.8	120.8
730	113.9	117.9	120.9
735	114.2	118.1	121.2
740	114.4	118.6	121.5
745	114.5	118.5	121.6
750	114.6	118.5	121.9
755	114.7	118.7	122.0
760	114.8	119.0	122.4
765	114.8	119.1	122.1
770	114.9	118.9	122.3
775	114.9	119.1	122.5
780	115.0	119.6	123.0
785	115.0	119.6	123.1
790	115.2	119.6	123.1
795	115.2	119.9	123.2
800	115.2	119.9	123.2

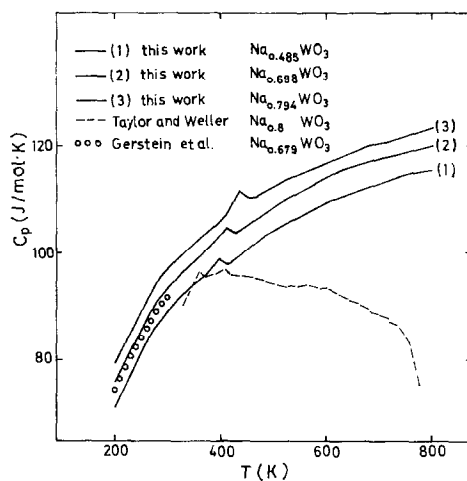


FIG. 1. Specific heats of $\text{Na}_{0.485}\text{WO}_3$, $\text{Na}_{0.698}\text{WO}_3$, and $\text{Na}_{0.794}\text{WO}_3$ with the results of $\text{Na}_{0.679}\text{WO}_3$ by Gerstein et al. and those of $\text{Na}_{0.8}\text{WO}_3$ by Taylor and Weller.

is within $\pm 1\%$. Data by Gerstein et al. are in good agreement with our results, taking into consideration the small difference of the sodium content of samples, but results by Taylor and Weller measured by DSC may contain large error at higher temperatures.

As discussed in previous papers (5, 13), in dynamic calorimeters a temperature difference is produced in the sample and a so-called scanning error is produced. The scanning error was corrected by shifting the sample temperature by about 3°K in this experiment according to the earlier method (5, 13).

Specific heats of Na_xWO_3 per gram-atom (per $1/(4+x)$ mole) at temperatures 200, 500, 600, 700, and 800°K , which have nothing to do with the phase transition, are given in

TABLE II
SPECIFIC HEAT OF Na_xWO_3 PER GRAM-ATOM
($1/(4+x)$ MOLE)

T ($^\circ\text{K}$)	Specific heat (J/g-atom \cdot K)		
	$\text{Na}_{0.485}\text{WO}_3$	$\text{Na}_{0.698}\text{WO}_3$	$\text{Na}_{0.794}\text{WO}_3$
200	15.88	16.05	16.52
500	23.23	23.03	23.47
600	24.33	24.22	24.28
700	25.06	25.03	25.07
800	25.69	25.52	25.70

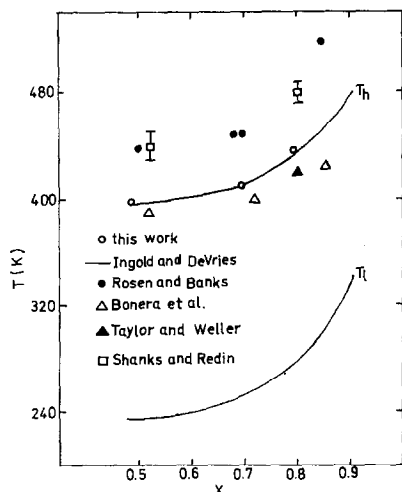


FIG. 2. Transition temperatures of Na_xWO_3 against the sodium content of sample.

Table II. Specific heats per gram-atom at each temperature are the same within experimental error, except for the case of 200°K , regardless of the difference in composition among the samples. Above the Debye temperature, which Gerstein et al. (11) have determined to be 450°K for $\text{Na}_{0.679}\text{WO}_3$, specific heats per gram-atom approach the Dulong-Petit value of 24.95 J/g-atom K, and those at 700°K correspond to the Dulong-Petit value.

A λ -type specific heat anomaly of Na_xWO_3 , as seen in Fig. 1, begins around 250°K and peaks around 400°K , depending on the sodium content of the sample; this shows the occurrence of a second-order phase transition. The peak temperature (T_h) of the phase transition against the sodium content of the sample is shown in Fig. 2; the previous data reported in the literature are also shown for comparison. In Fig. 2 the data of T_h show considerable scatter, which may be ascribed to the differences in sample preparation and the method of measurement. The data of T_h obtained by this work are in good agreement with those by Ingold and DeVries by the optical measurement (6). T_l shown in Fig. 2 obtained by Ingold and DeVries (6) represents the temperature at which birefringent patterns begin to appear, and this corresponds to the temperature at which the specific heat curve begins to rise, as seen in Fig. 1.

In the measurement of ^{23}Na spin-phonon relaxation rate in Na_xWO_3 (8) some peaks are overlapped, perhaps showing the existence of some corresponding relaxation mechanisms. But these effects may not clearly contribute to the specific heat curve.

To obtain the enthalpy and entropy changes due to the phase transition, the baseline of the specific heat curve for each sample of Na_xWO_3 is determined by the least-squares method, using the data in the range from 200 to 240°K and from 420 to 550°K (dependent on the sodium content of the sample) which have nothing to do with the specific heat anomaly, so as to fit the equation

$$C_p = a + bT - cT^{-2}.$$

By using the baseline thus determined, enthalpy and entropy increments for the

TABLE III
 ENTHALPY AND ENTROPY INCREMENT; AND THE
 TRANSITION TEMPERATURE FOR THE λ -TYPE
 TRANSITION IN Na_xWO_3

	ΔH (J/mole)	ΔS (J/mole·K)	T_h (°K)
$\text{Na}_{0.485}\text{WO}_3$	263 ± 9	0.79 ± 0.03	395
$\text{Na}_{0.698}\text{WO}_3$	289 ± 11	0.84 ± 0.04	410
$\text{Na}_{0.794}\text{WO}_3$	332 ± 12	0.90 ± 0.04	435

transition are obtained and are given in Table III, where the transition temperature T_h is also given.

T_h tends to increase as ΔH increases, and RT_h is plotted against ΔH as shown in Fig. 3, where good linearity is observed. This indicates that thermal energy necessary to cause the phase transition is related to the enthalpy change as the result of the transition. Similar behavior is seen in the phase transition of some nonstoichiometric compounds such as U_4O_{9-y} (5). The fact that T_h and enthalpy increments increase as the sodium content of the sample increases may indicate that the crystal structure becomes more stable as the sodium content increases.

Ingold et al. (6) supposed that before the transition the low temperature phase was distorted cubic (tetragonal) and the high temperature phase became cubic after the transition, judging from the analogy of the optical behavior with the phase transition of

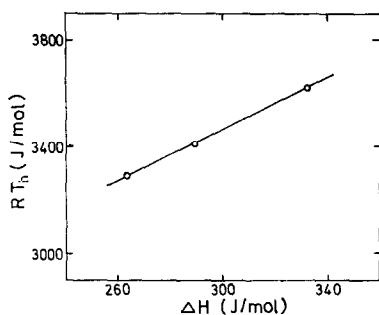


FIG. 3. Transition temperatures multiplied by gas constant against the enthalpy increments for the transition.

BaTiO_3 . The positive entropy change as shown in Table III may indicate that the crystal structure in the high temperature phase is more irregular than that in the low temperature phase. Atoji and Rundle (14) have found from the neutron diffraction study of Na_xWO_3 in the low temperature phase that oxygen atoms are slightly displaced with respect to the ideal perovskite structure, although the crystal structure differs little from the regular perovskite structure. It is supposed that the entropy change relates to the change of the number of such displaced oxygen atoms.

Although the detail of the phase transition of Na_xWO_3 has not been clear, the entropy change obtained in this study may be explainable by this supposition qualitatively. The positive entropy change indicates that the number of displaced atoms in the high temperature phase is more than that in the low temperature phase. This is supported by the fact (10) that the thermal conductivity in the high temperature phase is lower than that in the low temperature phase because the phonon scattering is increased in the high temperature phase by the increase of displaced atoms.

The fact that entropy increments increase as the sodium content of the sample increases is interpreted to mean that the number of displaced atoms from the ideal perovskite structure increases as the sodium content increases. This interpretation is also supported by the observation (10) that the decrease of the thermal conductivity of $\text{Na}_{0.804}\text{WO}_3$ during the transition is larger than that of $\text{Na}_{0.513}\text{WO}_3$.

References

1. L. D. ELLERBECK, H. R. SHANKS, P. H. SIDLES, AND G. C. DANIELSON, *J. Chem. Phys.* **35**, 298 (1961).
2. A. E. WHITEMAN, J. J. MARTIN, AND H. R. SHANKS, *J. Phys. Chem. Solids* **32**, 2223 (1971).
3. F. GRØNVOLD, *Acta Chem. Scand.* **24**, 1036 (1970).
4. F. GRØNVOLD, *Acta Chem. Scand.* **22**, 1219 (1968).
5. H. INABA AND K. NAITO, *J. Nucl. Mater.* **49**, 181 (1973).
6. J. H. INGOLD AND R. C. DeVRIES, *Acta Met.* **6**, 736 (1958).

7. C. ROSEN, B. POST, AND E. BANKS, *Acta Cryst.* **9**, 477 (1956).
8. G. BONERA, F. BONERA, M. L. CRIPPA, AND A. RIGAMONTI, *Phys. Rev.* **B4**, 52 (1971).
9. B. E. TAYLOR AND P. F. WELLER, *J. Solid State Chem.* **1**, 210 (1970).
10. H. R. SHANKS AND R. D. REDIN, *J. Phys. Chem. Solids* **27**, 75 (1966).
11. B. C. GERSTEIN, A. H. KLEIN, AND H. R. SHANKS, *J. Phys. Chem. Solids* **25**, 177 (1964).
12. B. W. BROWN AND E. BANKS, *J. Am. Chem. Soc.* **76**, 963 (1954).
13. K. NAITO, H. INABA, M. ISHIDA, Y. SAITO, AND H. ARIMA, *J. Phys. E* **7**, 464 (1974).
14. M. ATOJI AND R. E. RUNDLE, *J. Chem. Phys.* **32**, 627 (1960).